TECHNICAL REPORT: CVEL-06-001

AN IMPROVED MODEL FOR REPRESENTING CURRENT WAVEFORMS IN CMOS CIRCUITS

Yan Fu[1], Gian Lorenzo Burbui[2], and Todd Hubing[3]

[1]University of Missouri-Rolla
[2]University of Bologna
[3]Clemson University

October 12, 2006

A version of this report was submitted and later published in the *Proc. of the 18th International Zurich Symposium on Electromagnetic Compatibility*, Munich, Germany, Sep. 2007, pp. 289-292.

EXECUTIVE SUMMARY

A resistance-inductance-capacitance (RLC) model is described for estimating current waveforms in digital CMOS circuits. The model is based on parameters that are readily derived from information available in board layout files and component data sheets or IBIS files. Compared with the simpler triangular waveform traditionally used to approximate current in CMOS circuits, the RLC model more accurately estimates the shape of the current waveform in the time domain and the amplitudes of the upper harmonics in the frequency domain.

I. INTRODUCTION

Estimating the radiated EM emissions or crosstalk due to signals on a printed circuit board requires an estimate of the signal current. Normally, more emphasis is placed on modeling and controlling the voltage waveform in digital circuits. For binary digital signals, the voltage waveform alternates between a high and low level. However the current waveform can look very different, particularly in CMOS circuits with a capacitive load. T. Van Doren introduced a simple triangular pulse waveform model for estimating power-bus noise currents in CMOS circuits for an expert system evaluating emissions from PCB designs [1], which is shown in Figure 1.

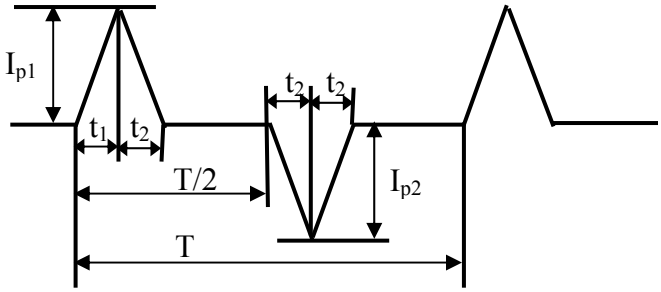

Fig. 1. Triangular model waveform for switching current.

J. Chen [2] and J. Mao [3] have applied this model to estimate power-bus noise due to multiple devices switching simultaneously. A similar model has been used by other researchers to estimate both signal and power currents [4]-[18]. For example, N. Na used triangular waveforms to model core switching currents [8][10]; L. Bouhouch used a similar waveform to model controller I/O switching currents [9]; and Kriplani employed a triangular waveform to model capacitive load currents [15].

The triangular waveform model has the advantage that it is based only on the amplitude and risetime of the voltage waveform. These parameters are generally readily available. However, this simple model does not do a good job of estimating the amplitude of the upper harmonics that are often very important when trying to anticipate or model a radiated emissions problem. Furthermore, with the advent of IBIS models and better simulation tools, information about the source and load impedances is often readily available. This makes it possible to obtain reasonably accurate current waveforms directly from voltage waveforms.

This paper explores the possibility of replacing triangular waveform current estimates with estimates based on a series RLC model for CMOS circuits. Simple formulas are derived for the current based on parameters that are normally available or readily estimated for CMOS circuits. The paper is organized as follows: Section II discusses the derivation of the new model. In Section III, new model calculations are compared with SPICE simulations. In Section IV, the measured current spectrum from a test board is compared with the new model and triangular model calculations.

II. RLC MODEL

A. Calculation of the current spectrum I(f).

The transient current drawn from a CMOS IC by a nearby CMOS load can be estimated using an RLC series equivalent circuit as shown in Figure 2. The voltage source and resistance represent the Thevenin equivalent model for the CMOS source. L represents the connection inductance between the source and load. C is the input capacitance of the receiving device.

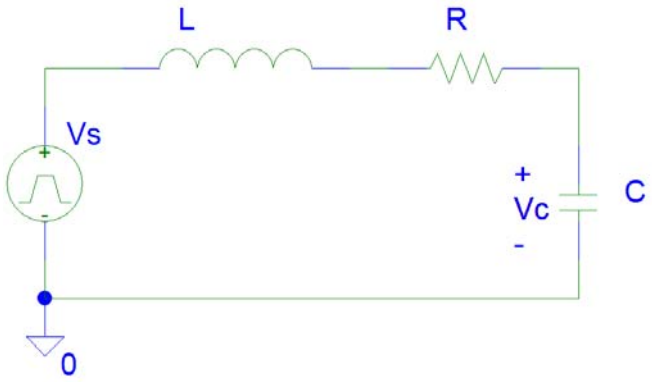

Fig. 2. Equivalent RLC circuit for a CMOS output gate and its load.

R can be obtained from IBIS voltage-current plots or estimated from the device data sheet as [19],

$$R \approx \frac{V_{CC} - V_{OH}}{I_{OUT}} \quad . \tag{1}$$

L depends on the geometry of the connection between the source and load. It can generally be estimated using simple closed-form formulas [20].

The voltage across the capacitor, V_C , can be determined by solving the second-order differential equation,

$$\frac{d^2V_C}{dt^2} + 2\xi\omega_n \frac{dV_C}{dt} + V_C = \omega_n{}^2 V_s \tag{2}$$

where ξ is the damping factor of the circuit,

$$\xi = \frac{1}{2Q} = \frac{R_1}{2\sqrt{L_1/C_1}} \tag{3}$$

and ω_n is the intrinsic resonance angular frequency of the circuit,

$$\omega_n = \frac{1}{\sqrt{L_1 C_1}}. \tag{4}$$

The load current is then given by

$$i_C = C\frac{dV_C}{dt}. \tag{5}$$

The step response of (5) is given by

$$i_C(t) = \begin{cases} \Delta V \dfrac{C_1\omega_n}{2\sqrt{\xi^2-1}}(e^{-(\xi-\sqrt{\xi^2-1})\omega_n t} - e^{-(\xi+\sqrt{\xi^2-1})\omega_n t})\cdot u(t), & \xi>1, \text{ or } 0<Q<0.5 \\ \Delta V \dfrac{1}{L_1} t e^{-t/\omega_n}\cdot u(t), & \xi=1, \text{ or } Q=0.5 \\ \Delta V \dfrac{C_1\omega_n}{\sqrt{1-\xi^2}} e^{-\xi\omega_n t}\sin\sqrt{1-\xi^2}\,\omega_n t\cdot u(t), & \xi<1, \text{ or } Q>0.5 \end{cases} \tag{6}$$

where $u(t)$ is the unit step function and ΔV is the amplitude of the source. The spectrum of the load current can be expressed in a simple closed form,

$$I(f) = \frac{2\Delta V}{j\omega}\frac{1}{R_1 + j\omega L_1 + 1/j\omega C_1}. \tag{7}$$

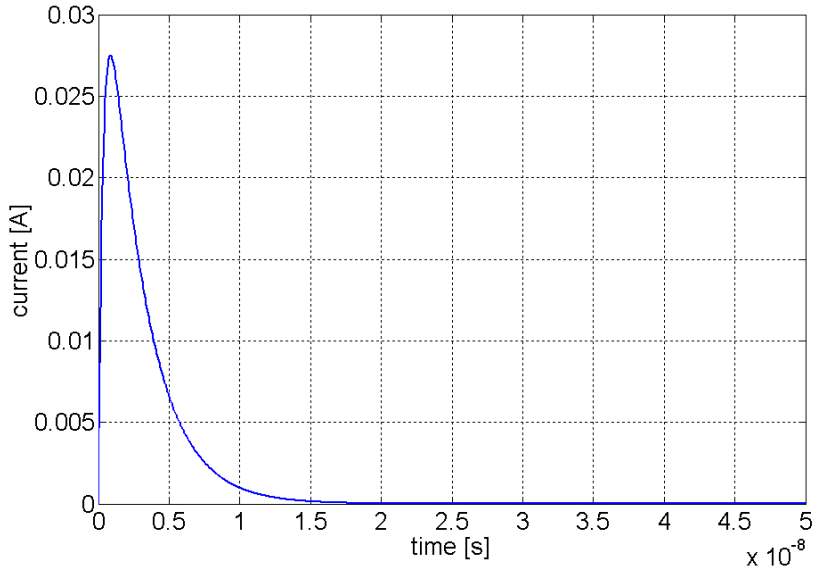

Fig. 3. RLC model in time domain ($0<Q<0.5$).

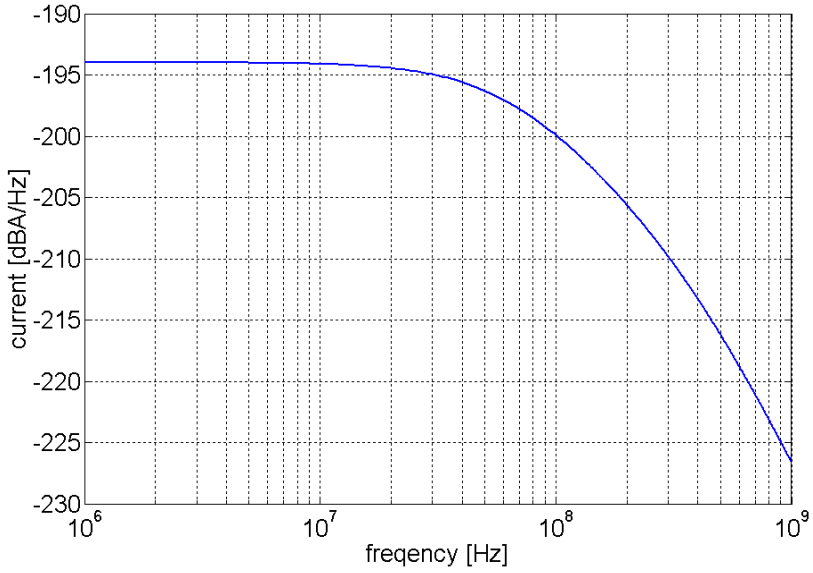

Fig. 4. RLC model spectrum ($0 < Q < 0.5$).

If $0 < Q < 0.5$, the circuit is over-damped. Fig. 3 and Fig. 4 show the time-domain waveform and the spectrum of the load current of an overdamped RLC circuit respectively. In this case, the component values were R=30 ohms, L=10 nH and C=100 pF. ΔV was 1 volt.

If $Q > 0.5$, the circuit is under-damped. An example of the current waveform and its spectrum for an underdamped circuit are shown in Fig's 5 and 6. In this case, the component values were R = 2 ohms, L = 10 nH and C = 100 pF. ΔV was 1 volt.

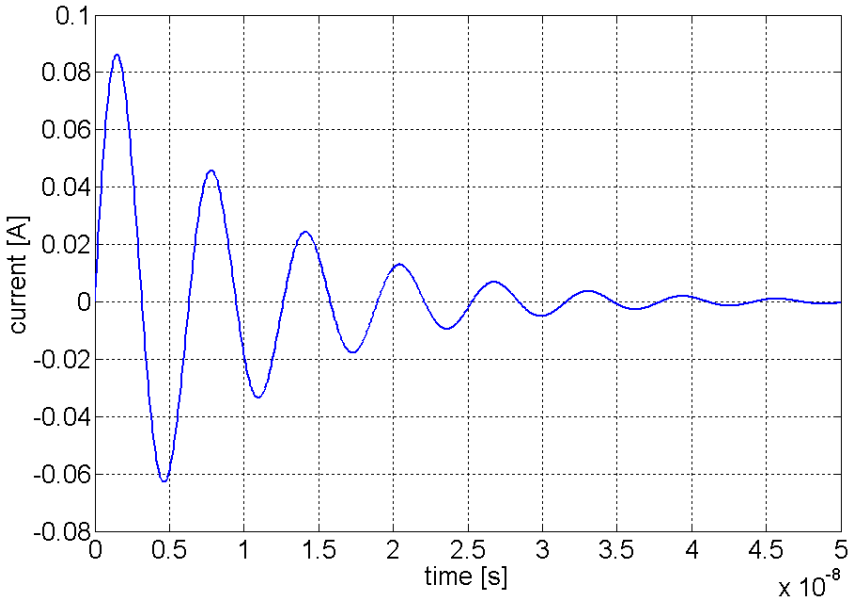

Fig. 5. RLC model in time domain ($Q > 0.5$).

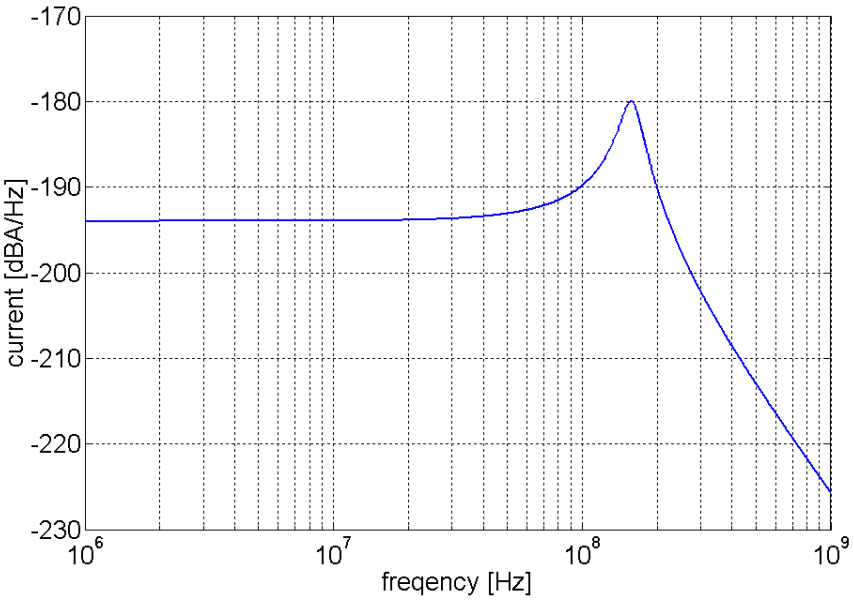

Fig. 6. RLC model spectrum ($Q > 0.5$).

When $Q = 0.5$, the circuit is critically-damped. An example of the current waveform and its spectrum for a critically-damped circuit are shown in Fig's 7 and 8. In this case, the component values were R = 20 ohms, L = 10 nH and C= 100 pF. ΔV was 1 volt.

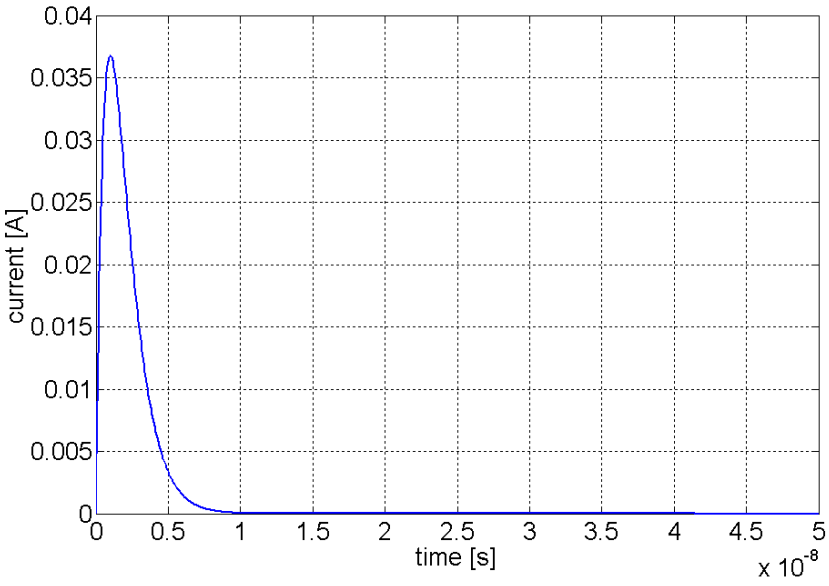

Fig. 7. RLC model in time domain ($Q = 0.5$).

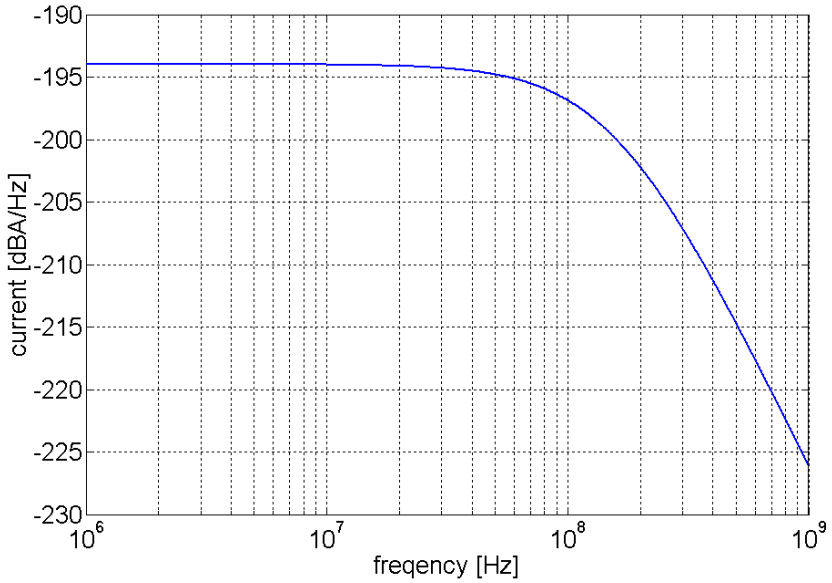

Fig. 8. RLC model in frequency domain ($Q = 0.5$).

B. Effect of finite source risetime

The transient current drawn by an IC device is also influenced by the source risetime. At high frequencies, finite risetimes cause harmonics of the source to fall off more rapidly. Practical models to estimate the current spectrum from CMOS sources above a few hundred MHz must take into account the finite risetime of the CMOS driver. The finite risetime of the voltage step supplying the RLC equivalent circuit can be accounted for in the frequency domain by simply multiplying by the source spectrum. For periodic trapezoidal waveforms, where T is the period of the voltage source and t_r is the rise and falltime of source; the magnitude of the current spectrum can be expressed as,

$$\left|I(nf_0)\right| = \frac{\left|V_S(nf_0)\right|}{\left|R_1 + j2\pi nf_0 L_1 + 1/j2\pi nf_0 C_1\right|} \tag{8}$$

where f_0 is the fundamental frequency of the voltage source and $V_S(nf_0)$ is the magnitude of the source spectrum which is given by,

$$\left|V_S(nf_0)\right| = \begin{cases} \dfrac{2\Delta V}{n\pi}, & n \le \dfrac{T}{\pi t_r} \\ \dfrac{2\Delta V}{(n\pi)^2}\dfrac{T}{t_r}, & n > \dfrac{T}{\pi t_r} \end{cases} \tag{9}$$

where n is an odd integer ≥ 1. We can obtain expressions for the envelope of the load current and source voltage by replacing nf_0 with f in Equations (8) and (9) respectively,

$$|I(f)| = \frac{|V_S(f)|}{\left| R_1 + j2\pi f L_1 + \frac{1}{j2\pi f C_1} \right|} \tag{10}$$

$$|V_S(f)| = \begin{cases} \frac{2}{T}\frac{\Delta V}{\pi f}, & f \le \frac{1}{\pi t_r} \\ \frac{2}{T}\frac{\Delta V}{(\pi f)^2}\frac{1}{t_r}, & f > \frac{1}{\pi t_r} \end{cases} . \tag{11}$$

Generally, it is better to calculate the envelope (maximum value) when estimating currents for EMC calculations, because small variations in the duty cycle can have a significant effect on the amplitude of individual upper harmonics.

III. Model Results vs. HSPICE Simulations

The formulas described in the previous section were validated using an HSPICE simulation tool to model the circuit in Fig. 2. Table 1 shows the parameters used for the simulations.

Table 1. Parameters used in the HSPICE simulations.

Parameters		Description	Value
t_r		Risetime of the voltage source	1 ns
Vcc		Amplitude of the voltage source	3.3 V
τ		Pulse width of the voltage source	50 ns
T		Period of the voltage source	100 ns
L_1		Parasitic inductance	10 nH
C_1		Load capacitance	100 pF
R_1	Case 1	under damped	5 ohms
	Case 2	over damped	20 ohms
	Case 3	critically damped	50 ohms

Fig's 9 - 11 compare the simulated current spectra using HSPICE to the calculated current envelope obtained using Equations (10) and (11). The odd harmonics are significantly higher than the even harmonics due to the fact that the pulse width is exactly half the period. Fig. 9 shows the case where the circuit is under-damped with a quality factor of 2. Fig. 10 shows the case where the circuit is critically damped. Fig. 11 shows the case where the circuit is over-damped, with a quality factor of 0.2. In each case, the model calculations accurately plot the envelope of the simulations. Both the HSPICE simulations and model calculations show that the envelope of the current spectrum has a slope of 60 dB/decade at high frequencies. This is due to the combined effects of the finite source risetime and the 40-dB/decade fall off of the LC circuit.

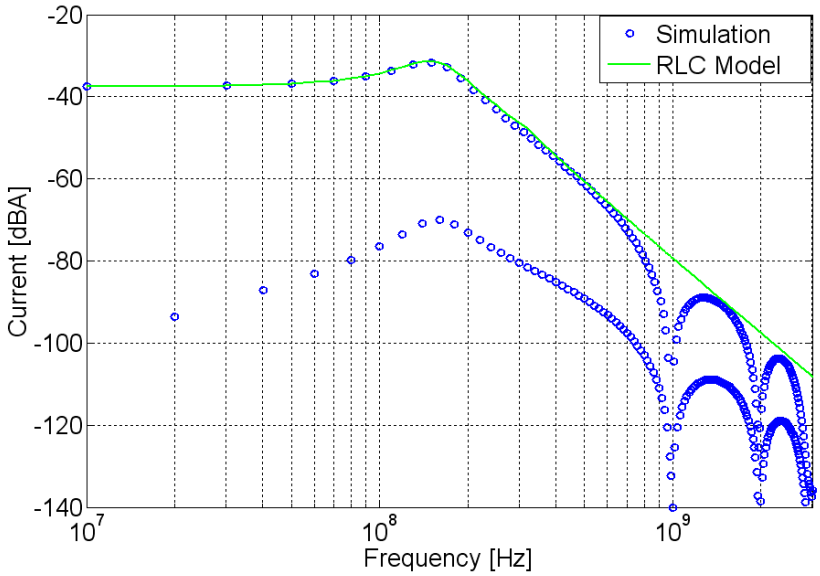

Fig. 9. Comparison of Spice simulation and RLC model calculation, Case 1: Q = 2.

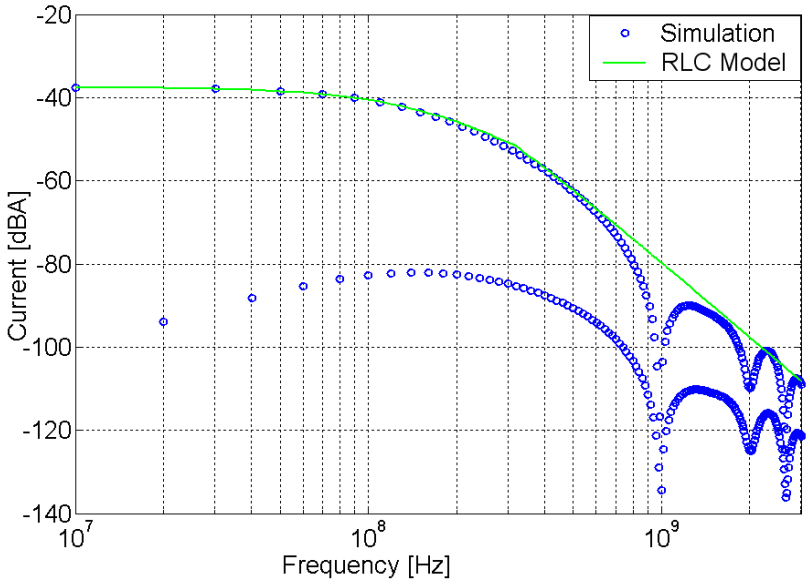

Fig. 10. Comparison of Spice simulation and RLC model calculation, Case 2: Q = 0.5.

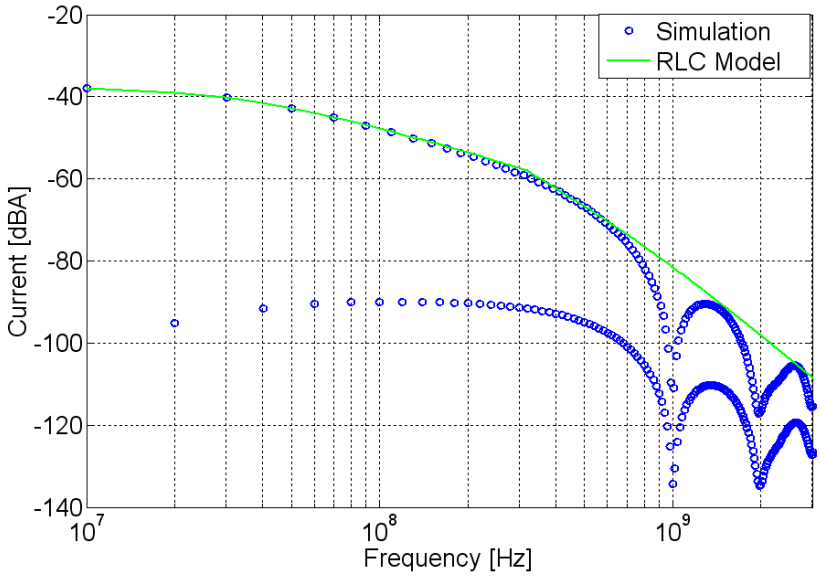

Fig. 11. Comparison of Spice simulation and RLC model calculation, Case 3: Q = 0.2.

IV. Model, Measurement, and Triangular Approximation Results

A. Measurement Setup

The expression for maximum estimated current in Equations (10) and (11) was evaluated experimentally and compared to the triangular approximation. Fig. 12 shows the equivalent circuit used for these comparisons. A CMOS clock buffer was driven by a signal source (a 50-MHz oscillator) and was loaded with capacitors of different values. A 2-ohm resistor was connected in series with the load capacitor in order to measure the load current. The parasitic inductance of the load interconnect was about 10 nH. The turn-on resistance of the CMOS buffer was about 4 ohms; therefore the total series resistance was about 6 ohms. The circuit was implemented on a 7.6-cm by 5.0-cm six-layer circuit board.

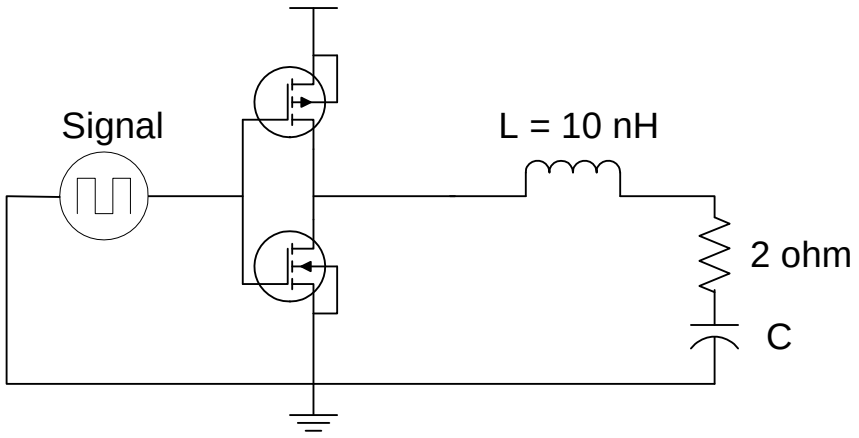

Fig. 12. Equivalent circuit of the measurement setup.

B. Results

1) Case 1. C = 10 pF.

Figure 13 shows the measured load current waveform (obtained by measuring the voltage across the 2-ohm resistor with an oscilloscope and dividing the voltage by 2-ohms) when the load capacitance was 10 pF. The quality factor of the circuit was about 5.3 (i.e. under damped). Fig. 14 shows the spectrum of the measurement (obtained using a spectrum analyzer) and envelope estimates obtained using Equations (10) and (11) and the triangular waveform model. The pulse width is approximated as a half of the ringing period in the triangular model calculation, $\Delta t = \pi\sqrt{LC}$. In the RLC model calculation, the risetime of the source signal ($t_r \approx 0.8$ ns) was obtained from an IBIS model [21]. The figure shows that the RLC calculation provides a better estimate of the envelope of the measured current spectrum than the triangular model. This is especially true at the upper harmonic frequencies. Fig. 14 shows that both the measurement and RLC model calculation show a 60-dB/decade slope at high frequencies, while the triangular model predicts a 40-dB/decade slope at high frequencies. The triangular model is not able to account for the combined effect of the finite source risetime and LC filtering.

2) Case 2. C = 100 pF.

Fig. 15 shows the measured current waveform when the load capacitance was 100 pF. In this case, the quality factor of the circuit was about 1.7 and the circuit was only slightly underdamped. Fig. 16 compares the measurement to the calculations using the RLC and triangular models. Again, the new model provides a better estimate of the envelope than the triangular model.

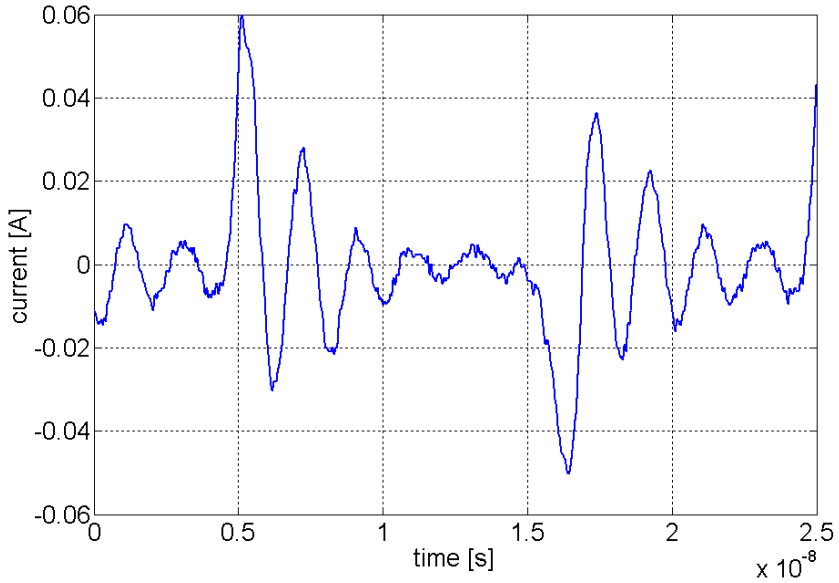

Fig. 13. Current waveform when C = 10 pF and R = 5 ohms.

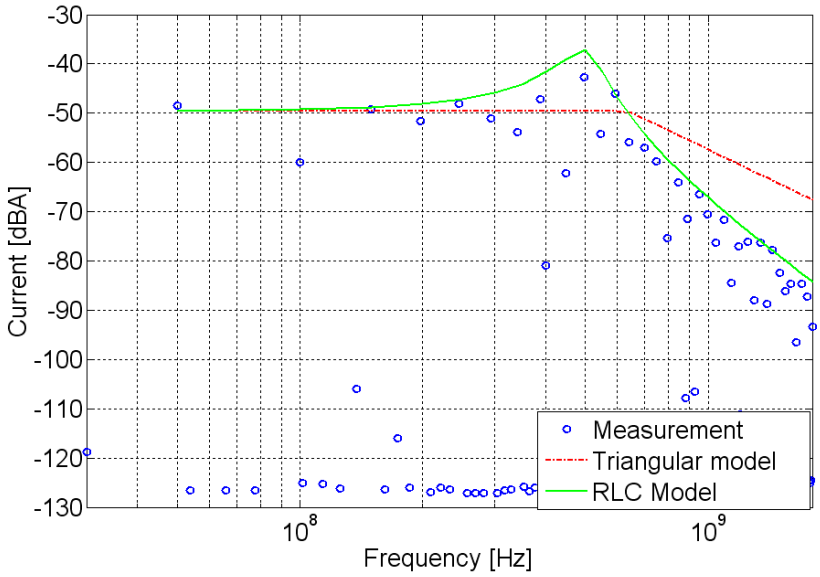

Fig. 14. Comparison of measurement, RLC model and triangular model calculation when C = 10 pF and R = 5 ohms.

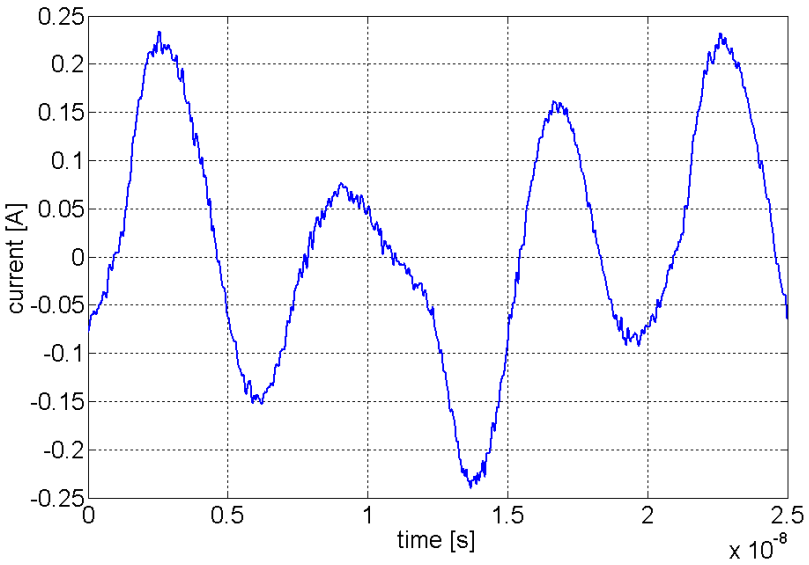

Fig. 15. Current waveform when C = 100 pF and R = 5 ohms.

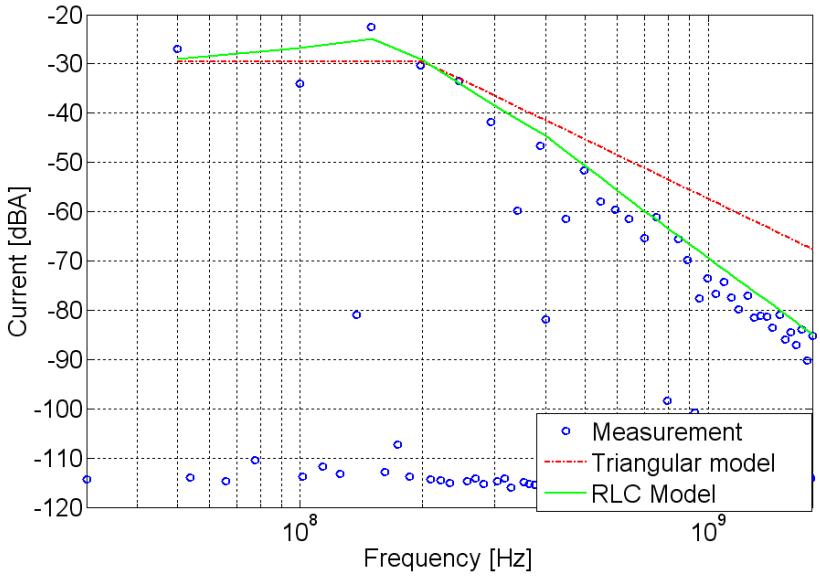

Fig. 16. Comparison of measurement, RLC model and triangular model calculation when C = 100 pF and R = 5 ohms.

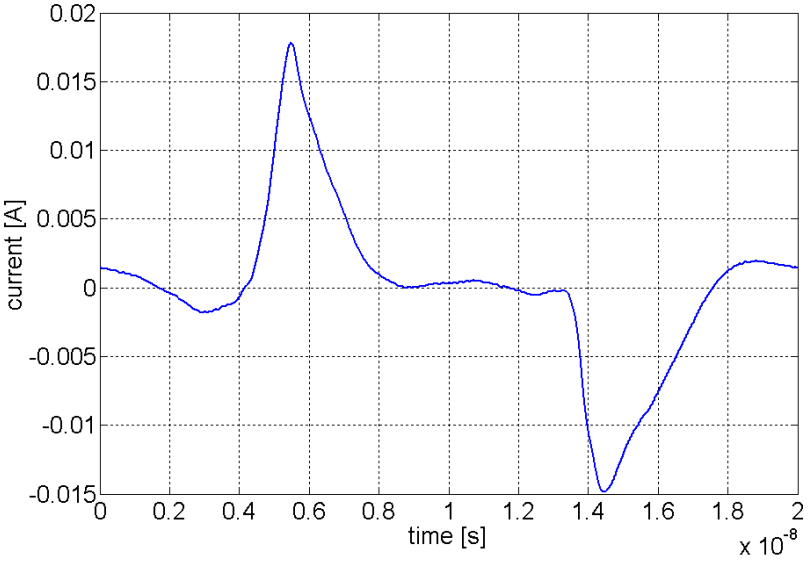

Fig. 17. Current waveform when C = 10 pF and R = 100 ohms.

3) Case 3: C = 10 pF, R = 100 ohms.

Figure 17 shows the measured current waveform when the load capacitance was 10 pF and the damping resistance was 100 ohms. In this case, the quality factor of the circuit was about 0.32. This is a slightly over-damped case. Figure 18 shows spectrum of the measurement and estimations using the RLC and triangular waveform models. For the triangular model, the risetime of the current was estimated as *2.2RC* (about 2.2 ns). The new model provides a better estimate of the envelope of the measured current spectrum than the triangular model estimation. The triangular estimate cut-off frequency is a little low, causing the upper harmonics to be under-estimated.

4) Case 4: Current delivered to an active device.

The current delivered to an actual CMOS device was also measured. The Philips 74LCX16244 line driver IC has 16 outputs, which were connected in parallel and driven by another 74LCX16244 line driver IC. The input capacitance of each line driver (~ 7 pF) was obtained from the data sheet. Therefore, the total input capacitance of the buffer IC was about 112 pF. The interconnect inductance associated with the trace between the driver and receiver was estimated to be 6 nH using the technique described in [20]. The total resistance was about 16 ohms. In this case, the quality factor of the circuit was about 0.45. Figure 19 shows the current waveform. Figure 20 shows spectrum of the measurement and estimates of the envelope obtained using the RLC and triangular waveform models. For the triangular model, the risetime of the current was estimated as *2.2RC* (about 4 ns). The RLC model provides a better estimate of the envelope of the measured current spectrum than the triangular model estimation.

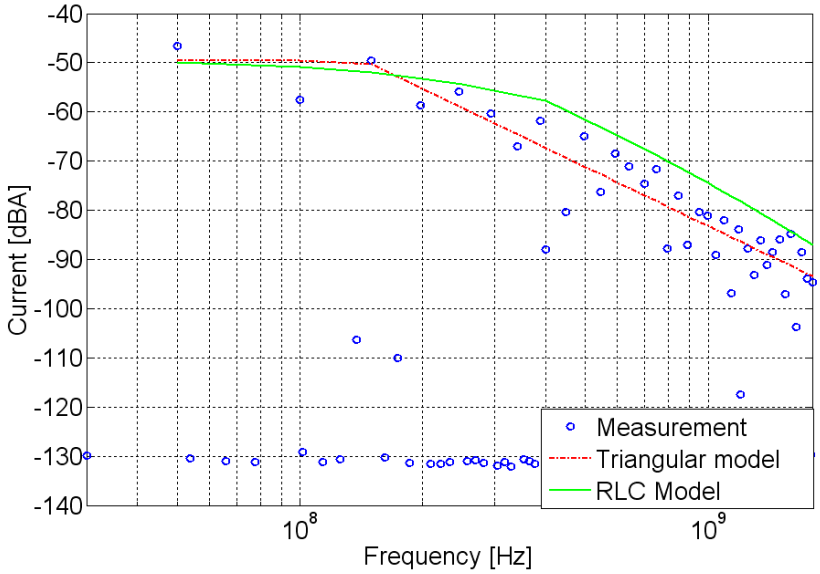

Fig. 18. Comparison of measurement, RLC model and triangular model calculation when C = 10 pF and R = 100 ohms.

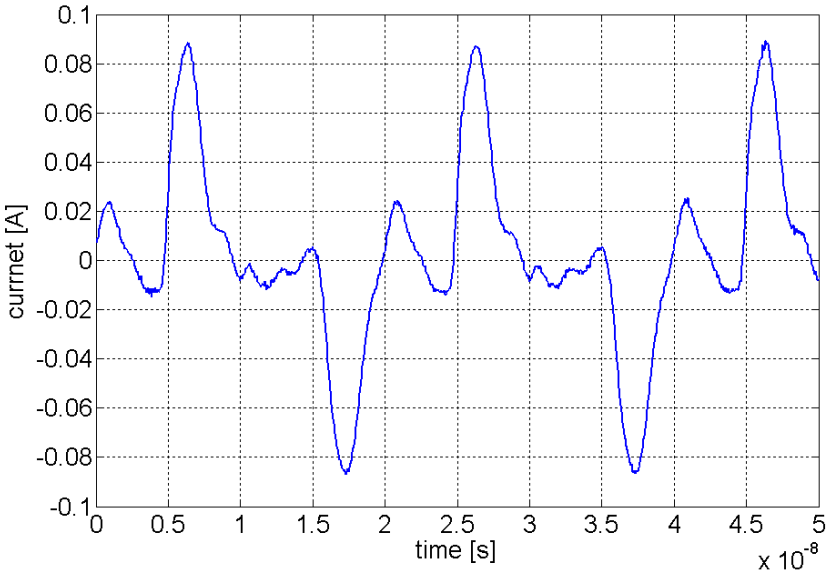

Fig. 19. Current waveform for an active device.

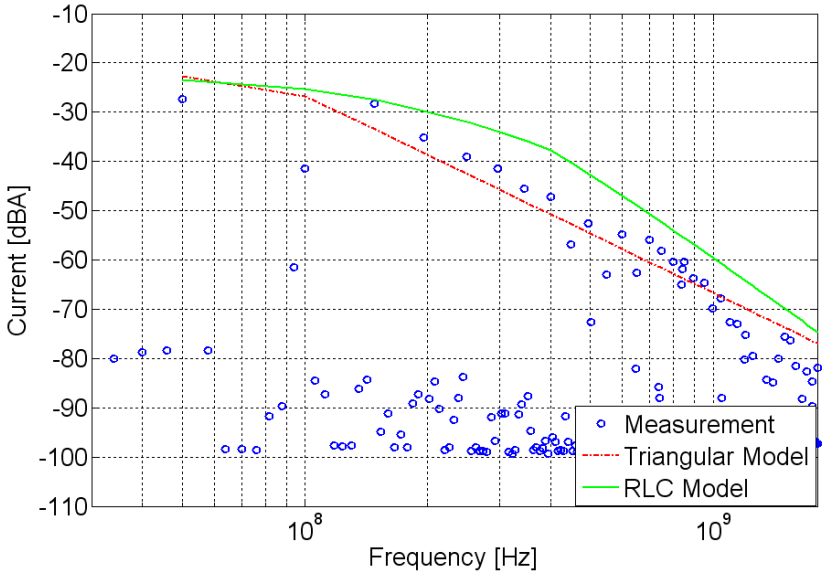

Fig. 20. Comparison of measurement, RLC model and triangular model calculation for active device current when C = 112 pF, L = 6 nH and R = 16 ohms.

V. CONCLUSIONS

The current spectrum calculated using closed-form formulas based on an RLC model was compared to simulations, measurements and triangular waveform model results. The RLC model provides a better estimate of the current spectrum than the triangular model, especially at upper harmonics. The RLC model predicts the 60dB/decade fall-off of the upper harmonics shown in both simulations and measurements, while the triangular model predicts a 40-dB/decade fall-off. Parameters required for the RLC model calculations are readily obtained from information available in board layout files and component data sheets or IBIS files.

REFERENCES

[1] T. Van Doren, "Expert System Power Bus Noise Algorithm", *University of Missouri-Rolla EMC Laboratory Technical Report TR99-3-024*, May 1999, http://www.emclab.umr.edu/consortium/technical.html.

[2] J. Chen, "Power Bus Radiation Measurements and Modeling," *University of Missouri-Rolla EMC Laboratory Technical Report TR99-7-028*, Sep. 1999, http://www.emclab.umr.edu/consortium/technical.html.

[3] J. Mao, B. Archambeault, J. Drewniak and T. Van Doren, "Estimating DC power bus noise," *Proc. 2002 IEEE Int. Symp. Electromag. Compat.*, Minneapolis, MN, Aug. 2004, pp. 1032-1036.

[4] IEC EMC Task Force. *IEC62014-3/Integrated Circuit Electromagnetic Model Cookbook* May 2002.

[5] P. Larsson, "Power supply noise in future IC's: A crystal ball reading," *Proc. of IEEE 1999 Custom Integrated Circuits Conference*, pp. 467-474, May 1999.

[6] H. H. Chen and J. S. Neely, "Interconnect and circuit modeling techniques for full-chip power noise analysis," *IEEE Trans. on Components, Packaging and Manufacturing Technology – Part B*, vol. 21, no. 3, pp. 209-215, Aug. 1998.

[7] K. Shimazaki, H. Tsujikawa, S. Kojima and S. Hirano, "LEMINGS: LSI's EMI-noise analysis with gate level simulator," *Proc. of IEEE 2000 First Int. Symp. on Quality Electronic Design ISQED'2000*, San Jose, CA, March 2000, pp. 129-136.

[8] N. Na, J. Choi, S. Chun, M. Swaminathan and J. Srinivasan, "Modeling and transient simulation of planes in electronic packages," *IEEE Trans. on Advanced Packaging*, vol. 23, no. 3, pp. 340-352, Aug. 2000.

[9] L. Bouhouch, M. Mediouni and E. Sicard, "Effects of microcontroller I/Os on conducted noise emission," *Proc. of EMC Compo 04*, Angers, France, April 2004, pp. 145-149.

[10] N. Na, J, Choi, M. Swaminathan, J. P. Libous and D. P. O'Connor, "Modeling and simulation of core switching noise for ASICs," *IEEE Trans. on Advanced Packaging*, vol. 25, no. 1, pp. 4-11, Feb. 2002.

[11] D. Panyasak, G. Sicard and M. Renaudin, "A current shaping methodology for low EMI asynchronous circuits," *Proc. of EMC Compo 02*, Toulouse, France, Nov. 2002, pp. 43-48.

[12] A. C. Deng, Y. C. Shiaunand K. H. Loh, "Time domain current waveform simulation of CMOS circuits," *ICCAD-88*, Santa Clara, CA, Nov. 1988, pp. 208-211.

[13] A. M. Martinez. "Quick estimation of transient currents in CMOS integrated circuits," *IEEE J. of Solid-State Circuits*, vol. 24, no. 2, pp. 520-531, April 1989.

[14] P. Vanoostende, P. Six and H. J. De Man, "PRITI: Estimation of maximal currents and current derivatives in complex CMOS circuits using activity waveforms," *Proc. of 4th European Conference on Design Automation with the European Event in ASIC Design*, Paris, France, Feb. 1993, pp. 347-353.

[15] H. Kriplani, F. Najm and I. Hajj, "Improved delay and current models for estimating maximum currents in CMOS VLSI circuits," *Proc. of ISCAS '94*, London, May 1994, pp. 435-438.

[16] J. H. Wang J. T. Fan and W. S. Feng, "An accurate time-domain current waveform simulator for VLSI circuits," *Proc. of European Design and Test Conference 1994,* Paris, Feb. 1994, pp. 562-566.

[17] A. Bogliolo, L. Benini, G. De Micheli and B. Ricco, "Gate-level current waveform simulation of CMOS integrated circuits," *Proc. of IEEE International Symposium on Low Power Electronics and Design*, Monterey, CA, Aug. 1996, pp. 109-112.

[18] H. Su, S. Sapatnekar and S. Nassif, "Optimal Decoupling capacitor sizing and placement for standard-cell layout designs," *IEEE Trans. on Computer-Aided Design of Integrated Circuits and Systems*, vol. 22, no. 4, pp. 428-436, Apr. 2003.

[19] H. W. Johnson, *High-Speed Digital Design*, PTR Prentice-Hall, Inc, 1996.

[20] T. Zeeff, "Estimating the Connection Inductance of a Decoupling Capacitor," *University of Missouri-Rolla EMC Laboratory Technical Report TR01-1-030*, June 2001, http://www.emclab.umr.edu/consortium/technical.html.

[21] IBIS (I/O Buffer Information Specification) ANSI/EIA-656-A website, Models link, http://www.eigroup.org/ibis/ibis table/models.htm.